

Biomolecular imaging using atomic force microscopy

Daniel J. Müller and Kurt Anderson

Atomic force microscopy (AFM) has become a well-established technique for imaging single biomacromolecules under physiological conditions. The exceptionally high spatial resolution and signal-to-noise ratio of the AFM enables the substructure of individual molecules to be observed. In contrast to other methods, specimens prepared for AFM remain in a plastic state, which enables direct observation of the dynamic molecular response, creating unique opportunities for studying the structure–function relationships of proteins and their functionally relevant assemblies. This review presents recent advances in methods and applications of AFM to imaging biological samples. It is clear that AFM will become an increasingly important tool for probing both the structural and kinetic properties of biological macromolecules.

Since its introduction in 1986, the potential of atomic force microscopy (AFM) for investigating biological samples on a scale ranging from living cells to single molecules has been recognized [1]. In contrast to conventional biological imaging methods, specimens investigated by AFM can be in a native, unlabeled state and investigated in their native environment for several hours – or even days – without damage.

The AFM raster scans a sharp, cantilever-mounted stylus over the specimen, thereby creating a 3D surface map. The relative stiffness and mobility of the specimen is an important limiting factor in the sensitivity of AFM to surface-position detection. In solid state materials, excellent signal-to-noise (S/N) ratios that enable the detection of stationary single atoms can be achieved. By contrast, biological specimens are soft and mobile – comparable to a water-filled sponge – and thus the force applied to the stylus must be kept very low to prevent sample deformation during AFM imaging. Likewise, topographs must be recorded in sufficiently short time ranges to prevent ‘blurring’ of the image caused by specimen movement. Here, we consider recent progress in using AFM for imaging single proteins in their native environment, observing proteins at work, the fast imaging of proteins, and the simultaneous determination of protein structure and multiple biochemical parameters.

Imaging of single native proteins

High-resolution AFM topography of native biological macromolecules is usually performed on proteins assembled into 2D crystals. Such crystals were originally developed to determine 3D protein structure by electron microscopy, and they serve as a good standard for assessing improvements in AFM sample preparation [2–4] and imaging conditions [5,6]. Comparisons of AFM topographs with protein structures determined by electron microscopy and

X-ray crystallography have shown excellent agreement within a lateral resolution of <1 nm and a vertical resolution of ~0.1 nm [7–9]. It can be concluded that the protein structures were not influenced by their adsorption to the supporting mica surface. The layered crystal mica is the most commonly used support for imaging of biological systems by AFM. It can be easily cleaved by an adhesive tape providing chemically inert and automatically flat surfaces over several hundreds of μm^2 . Interactions between sample and support must be carefully controlled in AFM sample preparation so that the integrity of fragile biological samples can be maintained [2]. More importantly, however, the exceptionally high S/N ratio of the AFM enables the identification of multiple alternative conformations that a protein can assume [7,10]. Classification of all conformational states observed for a given protein indicates probable transition pathways from one state to another. Interestingly, the local variability of protein structures observed by AFM correlates excellently with enhanced temperature factors found in structures determined by electron microscopy and with B-factors observed in structures determined by X-ray crystallography, which are interpreted as a measure of the amount of motion [8,11].

Single-molecule imaging at high resolution

Figure 1 shows sodium-driven rotors of the F_0F_1 ATP synthase from *Ilyobacter tartaricus* [12]. Because the rotors were embedded into a lipid membrane, they were sufficiently immobilized to be imaged at a lateral resolution of ~0.5 nm and a vertical resolution of ~0.1 nm. Each of the complete rotors consists of 11 subunits, which were clearly visible. In similar approaches, AFM has been used to determine the subunit stoichiometry of staphylococcal α -hemolysin [4], head-to-tail connectors of the $\phi 29$ bacteriophage [13], vacuolating toxin from *Helicobacter pylori* [14], and rotors from the chloroplast F_0F_1 ATP synthase [15]. The analysis

Daniel J. Müller* and Kurt Anderson

Max-Planck-Institute of Molecular Cell Biology and Genetics, Pfotenhauerstr. 108, D-01307 Dresden, Germany.

*e-mail: mueller@mpi-cbg.de

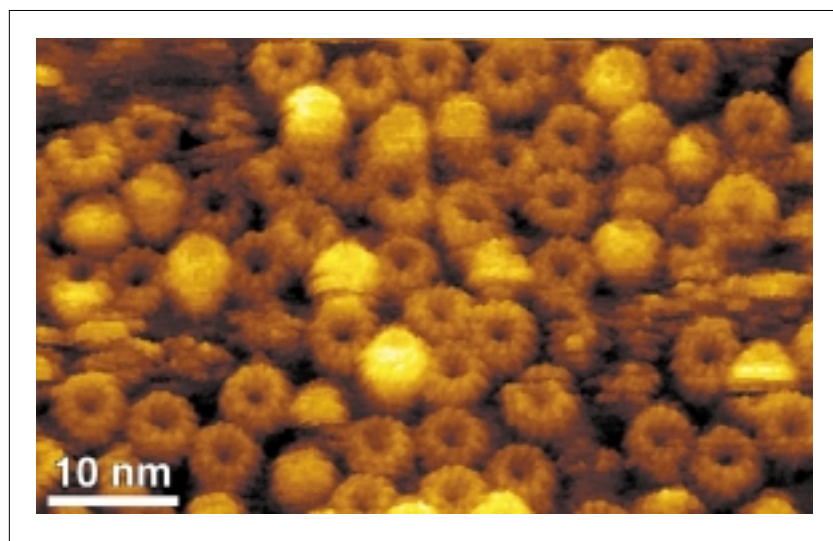


Figure 1. Assembly and stoichiometry of the sodium-driven rotor from *Ilyobacter tartaricus* ATP synthase

Reconstituted, densely packed rotors show an 11-fold symmetry. Wide and narrow rings represent the two aqueous surfaces of the membrane-spanning rotor. The topography was acquired in contact mode atomic force microscopy at applied forces of ~50–100 pN in buffer solution (10 mM Tris-HCl, pH 7.8, 300 mM KCl). It shows a full color scale corresponding to a vertical scale of 2.5 nm and is displayed as relief tilted by 5°.

of individual defective rotors missing one or several subunits has provided insight into how the subunits shape the final rotor and determine its stoichiometry [16]. Interestingly, the diffusion of rotors was not entirely suppressed by the adsorption of the membranes to the supporting mica surface. In addition, time-lapse AFM imaging could be used to observe the lateral and rotational diffusion of single rotors and to characterize their diffusion behavior (D.J. Müller et al., unpublished observations).

Structural identification

An important issue in microscopy is the positive identification of the object being imaged. One of the most common methods for identifying individual proteins and their surfaces is specific antibody labeling. This technique was used in combination with AFM to determine the structure of the cytoplasmic purple membrane surface of *Halobacterium salinarium* *in situ*, by injecting antibodies against a known surface marker into the liquid cell. Purple membrane consists of the light-driven proton pump bacteriorhodopsin and of lipid. The AFM tip was then used as a 'nanotweezer' to remove the antibody from the ligand and image the underlying structure at molecular resolution [17]. Alternative methods have been developed for identifying substructures of biological macromolecules. These include enzymatic removal of individual polypeptide loops or ends [18–20] and sequence substitution of loops with other polypeptides [20]. For these approaches, structural details were identified by comparing topographs recorded on native and modified proteins.

Observing proteins at work

Observing proteins in their native environment is a prerequisite for the proper assessment of function. Conformational changes of molecular assemblies can be observed

by time-lapse AFM; however, such experiments lack the time resolution required to observe the turnover of most biological 'machineries' owing to the relatively long time needed to record a topography (2–4 min). As described in this section, one solution to this problem is to image the static conformations associated with different functional states of a biological macromolecule. Alternatively, the imaging speed of the AFM can be enhanced.

Using the first approach, topographs of the inner surface of the surface layer from *Deinococcus radiodurans* were recorded by time-lapse AFM to reveal conformational changes of bacterial pores [7]. Individual pores reversibly switched from an open to a closed state independently of the conformation of neighboring bacterial pores. This example shows the strength of single-molecule techniques for observing the individuality of molecular biological processes.

The transmembrane channel-forming protein of *Escherichia coli*, OmpF porin, forms a large hollow β -barrel structure that perforates the outer membrane of the bacterium and enables the passage of ions and hydrophilic solutes. By using AFM, conformational changes – possibly associated with the gating of OmpF porin – were observed when an electrical potential was applied across the membrane. [7]. Aqueous domains of OmpF reversibly collapsed onto the membrane surface, thereby closing the channel entrance.

Connexons directly mediate cell-to-cell communication by connecting with connexons in neighboring cells, thereby bridging the extracellular space. Adding Ca^{2+} to the imaging buffer caused the connexons in rat liver epithelial cells to close, enabling this important protective mechanism to be imaged directly by AFM (Fig. 2) [21].

The transcription enzyme RNA polymerase moves along a DNA double helix to polymerize an RNA transcript. Using time-lapse AFM imaging, the displacement of DNA with respect to the RNA polymerase was observed after the addition of non-adenylic tri-phosphate (NTP) nucleotide [22]. The ability to observe directly such dynamic processes by AFM will enable the transcriptional process to be studied in great detail.

High-speed imaging of single proteins

Because of mechanical constraints of the AFM cantilever, the recording time of high-resolution topography of single molecules is currently a minimum of ~60 s. To speed up this scanning process, Hansma and colleagues devised soft and short AFM cantilevers that have a much higher resonance frequency of 130–200 kHz [23]. Using these cantilevers mounted to a fast-speed scanning AFM enabled the working cycle of the GroEL/GroES chaperonin system to be detected in buffer solution in the millisecond range,

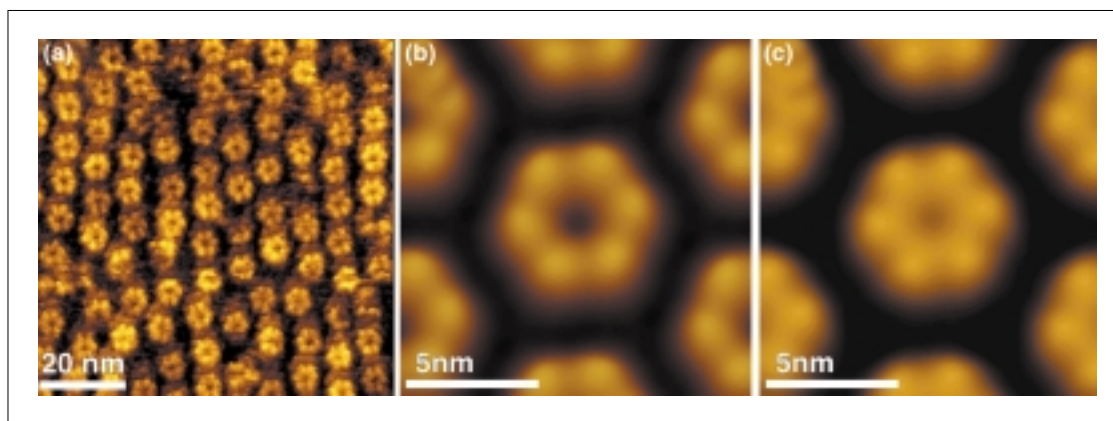


Figure 2. Ca^{2+} -induced conformational change of the extracellular connexon surface

(a) Extracellular connexon surface imaged in buffer solution (5 mM Tris, 1 mM EGTA and 1 mM PMSF). (b,c) Averaged topographs of extracellular connexon surfaces recorded in the absence (b) and presence (c) of 0.5 mM Ca^{2+} . These contact mode atomic force microscopy topographs were recorded using applied forces of 50 pN and a line frequency of 5.5 Hz. They are shown at a vertical scale of 2 nm.

with pico-Newton sensitivity [24]. The GroE machinery of *E. coli* mediates the folding of a large number of proteins *in vivo* and *in vitro*. GroEL and GroES were associated in the presence of 2.5 mM Mg-ATP, thereby forming a functional unit. This reversible binding and dissociation of GroEL and GroES was observed in real-time.

The interaction of substrate with the GroEL cavity can be assessed directly by coating the AFM tip with a substrate [25]. Interaction forces of citrate synthase from *Saccharomyces cerevisiae* and of RTEM β -lactamase from *E. coli* with GroEL, decrease in the presence of ATP but increase when the proteins are denaturated [25]. These and other examples of the GroE machinery show that AFM can be used to measure the interactions involved in protein folding, and that various functions of chaperonins in protein folding could be monitored at the single-molecule level.

Small cantilevers can be used with high-speed scanners to reduce significantly the recording time of native myosin molecules by a factor of ~300–400 [26] (Fig. 3). With this fast-speed AFM, 10–15 transitional states of a single molecule can be recorded within a second. However, most biological processes occur over much shorter time scales. Owing to the physical limitations of current cantilevers, new designs will be required to enable the conformational changes and dynamics of biological systems to be imaged in real-time and at high spatial and temporal resolution.

Simultaneous detection of structural and biochemical parameters

The combination of single-molecule imaging with other techniques to monitor topographical, biochemical and physical parameters simultaneously is a powerful, interesting and unique application of AFM. This correlation of biochemical and physical information can provide new insights into fundamental biological processes. Several different approaches for obtaining multiple parameters during AFM imaging have been developed, including AFM in combination with optical microscopy, patch

clamp electrophysiology [27], and ion-conductance pipettes [28]. Used as a sensor, the AFM tip can also be used to probe the charges of biological surfaces immersed in buffer solution [29–31]. So far, such approaches have successfully characterized protein interactions on the mesoscopic scale, but in the future they could be applied to imaging and detecting multiple parameters on a single molecule simultaneously.

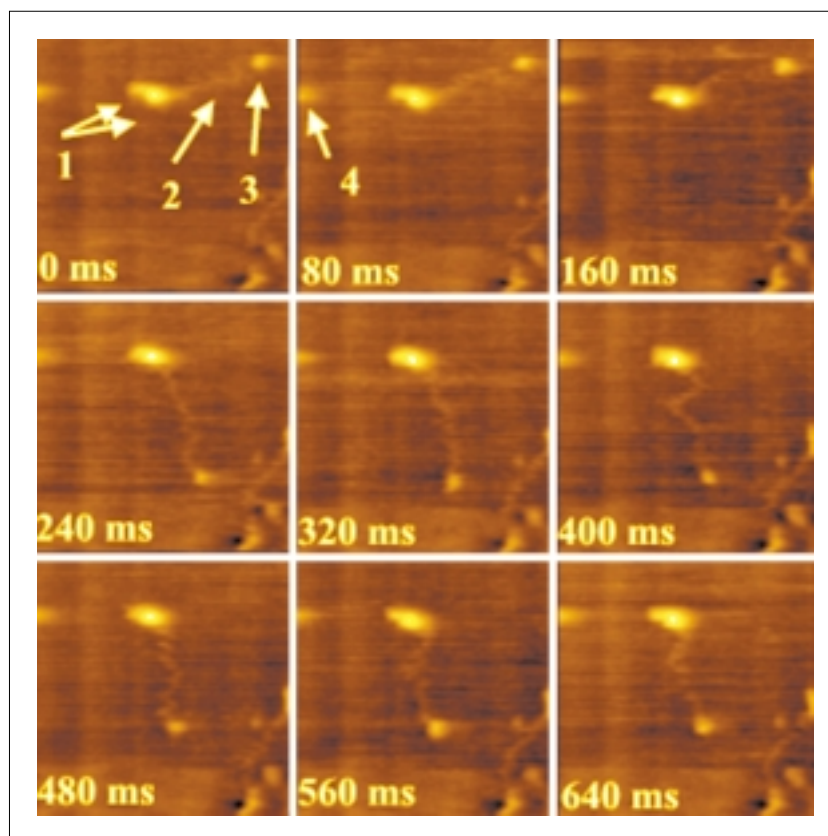
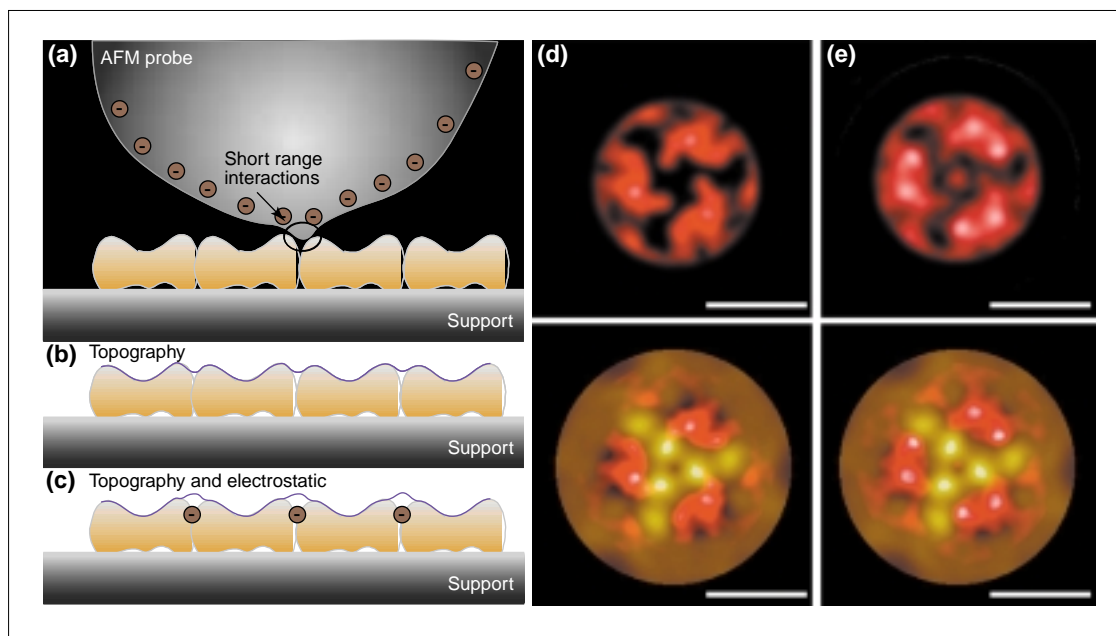


Figure 3. High-speed time-lapse atomic force microscopy images of myosin V adsorbed onto mica

The head/neck regions (1), the long tail (2) and the globular tail (3) are marked by arrows. After some topographs were recorded, the long tail and the globular tail changed their positions. A mirror image of one head region is marked with an arrow (4). The frames were imaged at a rate of 12.5 s^{-1} . Topographs, $240 \text{ nm} \times 240 \text{ nm}$, were recorded in 25 mM KCl, 25 mM Imidazole, 2 mM MgCl_2 , 2 mM ATP, 1 mM EGTA, at pH 7.2. (Image courtesy of Toshio Ando, Kanazawa University, Japan [26].)

Figure 4. Mapping the electrostatic potential of the OmpF porin channel

(a) Principle of recording topographs at variable electrostatic contribution. (b) Scanning a negatively charged atomic force microscope (AFM) tip (silicon nitride) over an electrically neutral surface reveals the true topography. (c) In the case of discrete negative charges, the AFM tip detects local electrostatic repulsions. The resulting topography represents a mixture of structural and electrostatic information, which can be decomposed by subtracting the topography recorded without electrostatic contributions from that recorded with electrostatic contributions. Difference maps between topographs of the periplasmic OmpF porin surface using 100 and 300 mM KCl (d) and at 50 and 300 mM KCl (e). The main differences between porin trimers recorded at different electrolyte concentrations are at the entrances of the transmembrane pore. The color scale from white (highest difference) to red (high difference <0.05 nm) corresponds to a vertical height of 0.3 nm (d) and of 0.5 nm (e). Lower panels show the superimposition of the averaged topography (colored brown-gold) and the electrostatic potential. Scale bars, 5 nm.



An initial step in this direction was taken with the recording by AFM of the electrostatic potential of transmembrane channels under variable electrostatic conditions [11]. The electrostatic potential established by porin OmpF was decomposed by subtracting topographs recorded at different strengths of electrostatic force (Fig 4a). The results show that porin establishes a negative electrostatic potential at its pore entrance, which increases with decreasing electrolyte concentration. This potential might be responsible for the pore selectivity against negatively charged ions. The bottom panels of Figs 4d and e show the superimposition of the AFM topography (brown-gold) and the electrostatic potential (red to white). The electrostatic potentials represent difference maps calculated from topographs recorded under different electrostatic conditions.

Future insights into biomolecular processes

AFM has become a well-established technique for imaging individual macromolecules at a spatial resolution of <1 nm. The next step will be to establish new AFM methods to investigate structure–function relationships among the variety of molecular machines. Such results will provide insights into how such machines work at the molecular level, and drive the understanding of common principles that govern them. The next challenge will be to study the behavior of individual molecular machines in heterogeneous assemblies, and to understand how different machines form small functional entities. Here, again, AFM promises to be an important tool as it enables individual molecules to be imaged at sufficient resolution for their behavior within macromolecular complexes to be characterized.

References

- Drake, B. et al. (1989) Imaging crystals, polymers, and processes in water with the atomic force microscope. *Science* 243, 1586–1588
- Amrein, M. and Müller, D.J. (1999) Sample preparation techniques in scanning probe microscopy. *Nanobiology* 4, 229–256
- Wagner, P. (1998) Immobilization strategies for biological scanning probe microscopy. *FEBS Lett.* 430, 112–115
- Czajkowsky, D.M. et al. (1998) Staphylococcal α -hemolysin can form hexamers in phospholipid bilayers. *J. Mol. Biol.* 276, 325–330
- Möller, C. et al. (1999) Tapping mode atomic force microscopy produces faithful high-resolution images of protein surfaces. *Biophys. J.* 77, 1050–1058
- Müller, D.J. et al. (1999) Electrostatically balanced subnanometer imaging of biological specimens by atomic force microscopy. *Biophys. J.* 76, 1101–1111
- Engel, A. and Müller, D.J. (2000) Observing single biomolecules at work with the atomic force microscope. *Nat. Struct. Biol.* 7, 715–718
- Heymann, J.B. et al. (1999) Charting the surfaces of purple membrane. *J. Struct. Biol.* 128, 243–249
- Baker, A.A. et al. (2000) New insight into cellulose structure by atomic force microscopy shows the α crystal phase at near-atomic resolution. *Biophys. J.* 79, 1139–1145
- Scheuring, S. et al. (2002) Sampling the conformational space of membrane protein surfaces with the AFM. *Eur. Biophys. J.* 31, 172–178
- Philippens, A. et al. (2002) Imaging the electrostatic potential of transmembrane channels: atomic probe microscopy on OmpF porin. *Biophys. J.* 82, 1667–1676
- Stahlberg, H. et al. (2001) Bacterial ATP synthase has an undecameric rotor. *EMBO Reports* 21, 1–5
- Müller, D.J. et al. (1997) The bacteriophage ϕ 29 head–tail connector imaged at high resolution with atomic force microscopy in buffer solution. *EMBO J.* 16, 101–107
- Czajkowsky, D.M. et al. (1999) The vacuolating toxin from *Helicobacter pylori* forms hexameric pores in lipid bilayers at low pH. *Proc. Natl. Acad. Sci. U.S.A.* 96, 2001–2006
- Seelert, H. et al. (2000) Proton powered turbine of a plant motor. *Nature* 405, 418–419
- Müller, D.J. et al. (2001) ATP synthase: constrained stoichiometry of the transmembrane rotor. *FEBS Lett.* 504, 219–222
- Müller, D.J. et al. (1996) Immuno-atomic force microscopy of purple membrane. *Biophys. J.* 70, 1796–1802
- Fotiadis, D. et al. (2000) Surface tongue-and-groove contours on lens MIP facilitate cell-to-cell adherence. *J. Mol. Biol.* 300, 779–789
- Scheuring, S. et al. (1999) High resolution topographs of the *Escherichia coli* waterchannel aquaporin Z. *EMBO J.* 18, 4981–4987
- Heymann, J.B. et al. (2000) Conformations of the rhodopsin third cytoplasmic loop grafted onto bacteriorhodopsin. *Structure* 8, 643–644

- 21 Müller, D.J. et al. Conformational changes in surface structures of isolated Connexin26 gap junctions. *EMBO J.* (in press)
- 22 Guthold, M. et al. (1999) Direct observation of one-dimensional diffusion and transcription by *Escherichia coli* RNA polymerase. *Biophys. J.* 77, 2284–2294
- 23 Viani, M.B. et al. (1999) Small cantilevers for force spectroscopy of single molecules. *J. Appl. Phys.* 86, 2258–2262
- 24 Viani, M.B. et al. (2000) Probing protein–protein interactions in real time. *Nat. Struct. Biol.* 7, 644–647
- 25 Vinckier, A. et al. (1998) Atomic force microscopy detects changes in the interaction forces between GroEL and substrate proteins. *Biophys. J.* 74, 3256–3263
- 26 Ando, T. et al. (2001) A high-speed atomic force microscope for studying biological macromolecules. *Proc. Natl. Acad. Sci. U.S.A.* 98, 12468–12472
- 27 Hörber, J.K.H. et al. (1995) A look at membrane patches with a scanning force microscope. *Biophys. J.* 68, 1687–1693
- 28 Proksch, R. et al. (1996) Imaging the internal and external pore structure of membranes in fluid: TappingMode scanning ion conductance microscopy. *Biophys. J.* 71, 2155–2157
- 29 Butt, H.-J. et al. (1995) Measuring surface forces in aqueous solution with the atomic force microscope. *Bioelect. Bioenerg.* 38, 191–201
- 30 Czajkowsky, D. et al. (1998) Direct visualization of surface charge in aqueous solution. *Ultramicroscopy* 74, 1–5
- 31 Heinz, W.F. and Hoh, J.H. (1999) Relative surface charge density mapping with the atomic force microscope. *Biophys. J.* 76, 528–538